^{237}Np absolute delayed neutron yield measurements

D. Doré[1,a], X. Ledoux[2], R. Nolte[3], F. Gagnon-Moisan[4], L. Thulliez[1], O. Litaize[5], S. Roettger[3], and O. Serot[5]

[1] Irfu, CEA, Université Paris-Saclay, 91191 Gif-sur-Yvette, France
[2] GANIL, 14000 Caen, France
[3] Physikalisch Technische Bundesanstalt, 38116 Braunschweig, Germany
[4] Paul Scherrer Institute, 5232 Villigen, Switzerland
[5] CEA, DEN, DER, Cadarache, 13108 Saint-Paul-lez-Durance, France

Abstract. ^{237}Np absolute delayed neutron yields have been measured at different incident neutron energies from 1.5 to 16 MeV. The experiment was performed at the Physikalisch-Technische Bundesanstalt (PTB) facility where the Van de Graaff accelerator and the cyclotron CV28 delivered 9 different neutron energy beams using p+T, d+D and d+T reactions. The detection system is made up of twelve ^{3}He tubes inserted into a polyethylene cylinder. In this paper, the experimental setup and the data analysis method are described. The evolution of the absolute DN yields as a function of the neutron incident beam energies are presented and compared to experimental data found in the literature and data from the libraries.

1. Introduction

Delayed neutrons and gamma-rays are emitted after the beta- decay of neutron-rich nuclei (called precursors). These nuclei are produced, for example, by the fission of actinides. Recent development of non-destructive methods for the detection of nuclear materials use the emission of neutrons (DN) to detect actinides by irradiating nuclear waste barrels or containers with photon or neutron beams.

Obviously, delayed neutrons (DN) play a crucial role in nuclear reactor control. For accelerator driven systems (ADS) with minor actinide contents, the DN balance is different from usual reactors. The neutron economy is strongly affected by the low DN yield of actinides to be transmuted. It is then necessary to know the energy dependence of minor actinide DN yields. Results found in the literature for ^{237}Np DN yields only cover a small domain in incident neutron energy. Since ^{237}Np is one the easiest nuclei to study in the minor actinide region, it was a motivation to perform measurements of DN yields with a high precision over a large energy domain. An experiment was then carried out at the ion accelerator facility PIAF of the Physikalisch-Technische Bundesanstalt (PTB) for nine neutron incident energies between 1.5 MeV and 16 MeV. The methodology, the facility and the experimental setup are presented in Sect. 2. The analysis method and corrections are described in Sect. 3. Results and interpretation are presented and discussed in Sect. 4.

2. Experimental scenario and setup

The experimental methodology is similar to the one presented in [1]. Here it was optimized taking into account the characteristics of ^{237}Np DNs found in the literature. These characteristics are the a_i and λ_i of the six DN groups. Indeed, the time-dependent yield of DN is generally expressed by the sum of six exponentials Eq. (1), each one representing a group of precursors.

$$Y_{\mathrm{d}} = n_{\mathrm{f}} \nu_{\mathrm{d}} \sum_{i=1,6} a_i \exp(-\lambda_i t)\,(1-\exp(-\lambda_i t_{\mathrm{irr}})) \quad (1)$$

Here

ν_d is the total number of delayed neutrons per fission,
a_i is the relative abundance of the group i, $\sum_{i=1}^{i=6} a_1 = 1$,
$\lambda_i = \ln(2)/T_i$ is the decay constant of the group i. with the mean half life T_i,
n_{f} is the fission rate,
t is the time relative to the end of irradiation.

For a long irradiation time (t_{irr}) the precursor concentrations approach an equilibrium and the second term of Eq. (1) tends to unity. Thus at $t = 0$ s, Eq. (1) can be rewritten

$$F_{\mathrm{det}}(0) = \epsilon \nu_d n_f \quad (2)$$

with ε, the detection efficiency and $F_{\mathrm{det}}(0)$ the detection rate. The ν_d is then deduced from the DN measurement at $t = 0$ s and the fission rate in the target. For this experiment, the scenario was an irradiation of 300 seconds to reach the equilibrium followed by a large number of periodic irradiation-decay cycles (7 s and 1 s respectively) to maintain the equilibrium and reach the needed statistics. During the decay, DNs are registered as a function of time.

2.1. Experimental setup

The experiment was performed at the PTB Ion Accelerator Facility PIAF in Braunschweig (Germany) [2]. Three different reactions (^{3}H(p,n)^{3}He, ^{2}H(d,n)^{3}He and ^{3}H(d,n)^{4}He) were used to produce neutron beams at nine different energies. Charged particles were delivered by the 3.75 MV Van de Graaff accelerator (VdG) or the CV28 cyclotron. A

[a] e-mail: diane.dore@cea.fr

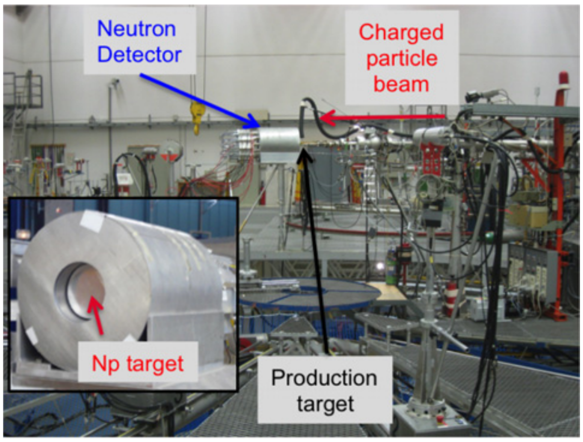

Figure 1. Picture of the experimental setup.

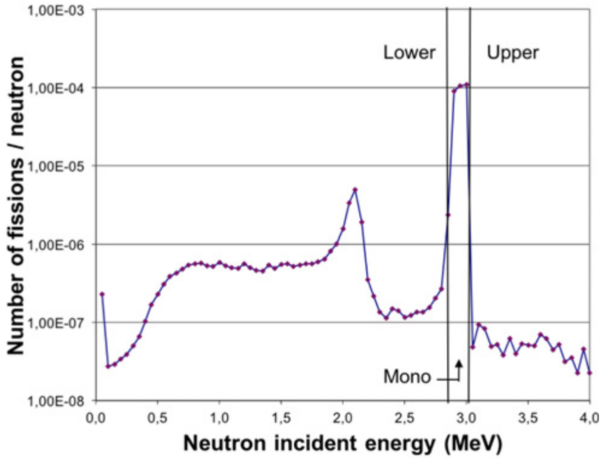

Figure 2. Number of fissions in ^{237}Np per incident neutron as a function of the incident neutron beam energy. The limits for the definition of "Lower", "Upper" and Mono contributions are shown. The high energy part of the spectrum is not shown but has been taken into account in the calculations of the number of fissions.

fast steering magnet was used to switch the beam on and off for the irradiation/decay. The beam deflection and the data acquisition system were synchronised by a clock. (see [1] for details).

The ^{237}Np target had a diameter of 80 mm and was 0.5 mm thick. It contained of (49.47 ± 0.27) g of ^{237}Np, (6.95 ± 0.28) g of ^{16}O and (0.27 ± 0.06) g of ^{232}Th. The neutron background produced by the target itself was measured. About 10 events/s were observed.

The experiment was performed in an open-field geometry, i.e. without collimator. The sample was placed close to the neutron production target at the entrance of the DN detector (see Fig. 1). Two different positions were used depending on the particular neutron producing reaction used. As explained in Sect. 3, this served to maximize the detection efficiency and minimize the impact of scattered neutrons on the sample.

The DN detector is made up of twelve ^{3}He counters (30 cm long with a diameter of 2.5 mm) at a pressure of 4 bars, embedded in a polyethylene cylinder of 37 cm long with inner and outer radii of 6 and 16 cm respectively. The cylinder is wrapped in a 1 mm cadmium foil to shield the detector from low energy background neutrons. The efficiency of the detection system for DN neutrons was simulated using the MCNPX software [3]. The full geometry of the experimental setup was implemented. A source of DN neutrons was distributed uniformly in the sample volume with a flat energy distribution between 0.1 and 1.0 MeV. The detector was designed to have an almost constant efficiency in this energy range. This is very important since the energy of the DNs is not measured. In addition, comparisons between simulations and measurements with a ^{252}Cf source placed at different positions were performed. The measured and simulated event rates were almost identical which proved that our simulations were relevant and that unsimulated effects were negligible. The efficiency of this ensemble was evaluated to be around 12% or 15% according to the two positions of the ^{237}Np sample in the detector. The efficiency is almost constant in the expected DN energy range.

For each beam energy, the neutron fluence per unit beam charge at the position of Np sample was determined in separate runs using a recoil proton proportional counter (neutron energies below 2 MeV), a recoil proton telescope (neutron energies above 5.9 MeV) or a de Pangher long counter at 0°. The energy of the neutrons was calculated from the beam energies and the energy loss in the neutron production targets. The beam charge Q and the event rate of a second de Pangher long counter mounted at 98° were used as monitors to related the fluence measurement to the measurement of the DN yield. Corrections for inscattering from the polyethylene moderator into the de Pangher long counter monitor were determined in separate runs with the DN detector moved to a remote position. The background produced by the scattering of neutrons in the polyethylene moderator or in the production target assembly was measured independently. A detailed explanation of the flux determination is found in [1].

3. Data analysis

The first step of the analysis was the summation of DN time distributions over the cycles of a run. $F_{\text{det}}(0)$, needed for the calculation of ν_d, was then determined by extrapolating the fit of the decay time spectrum. The function used for the fit is given in Eq. ((1)). Various ensembles of a_i and λ_i found in the literature were tested. The impact on the F_{det} value was small and were taken into account in the uncertainty calculations.

The number of fissions in the sample per incident neutron (N_f/n) was obtained from the MCNPX simulations. The total number of fissions in a run was obtained by multiplying N_f/n by the neutron fluence at the position of Np sample.

The number of fissions per incident neutron was calculated using MCNPX taking into account the full setup geometry (detector, sample thickness, ...). Since the experiment was performed in an open-field geometry, some neutrons were scattered in the polyethylene before impinging the target. Some other neutrons were scattered in the target before producing fission. There is also a higher energy component since neutrons produced by the Np fissions can trigger other fissions. All these contributions are shown in Fig. 2 for the 3 MeV incident energy run. Three energy domains have been defined: "mono", "upper"

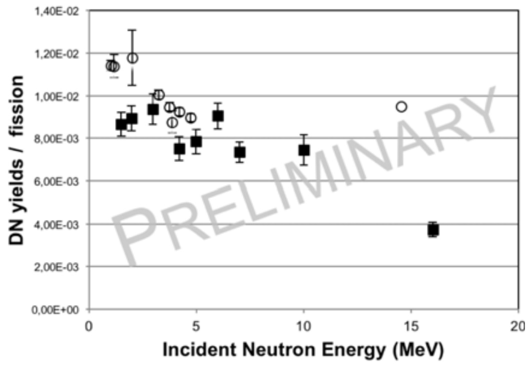

Figure 3. Delayed neutron yields per fission as a function of the incident neutron energy. Results from this work are the filled black squares and results found in the literature [4,5] are the open circles. ENDF/B-VII (solid line) and JEFF-3.2 (dotted line) dependences are superimposed.

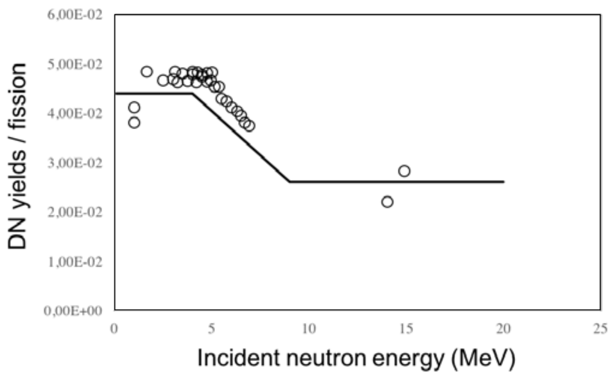

Figure 4. Delayed neutron yields per fission as a function of the incident neutron energy for ^{238}U. Results found in the literature [4] are the open circles. ENDF/B-VII (solid line) dependence is superimposed.

and "lower" for the contributions of direct neutrons, fission neutrons and scattered neutrons respectively.

Although the maximum number of fissions occurred at the beam energy (mono), the contributions from lower and upper parts had to be taken into account. The F_{det} value can be expressed by

where $N_{fission}$ are the fission rates in the different energy domains. ν^u and ν^d are the averaged delayed neutron yields in the upper and lower parts of the energy spectrum. A first estimation of these values was calculated with the present DN values obtained without any correction. An iterative procedure was applied in order to obtain final values for ν^u and ν^d. Then the ν^{mono} was determined. The DN contributions from the lower and upper parts were found to be very small compared to the beam energy contribution.

Finally, a method of propagation of uncertainties was applied through the DN yield calculations. In addition to the statistical uncertainties of the event rates and the uncertainty of the fluence measurements, uncertainties due to the fit, the detection efficiency, the ν^u and ν^d values and the sample mass were taken into account

4. Results and interpretation

Preliminary DN yields are shown in Fig. 3 for incident neutron beam energies between 1 MeV and 16 MeV. Results of this work (filled squares) are compared to results of the literature (open circles) [4,5]. Both sets of data show a smooth energy dependence. At low (<2 MeV) and high (16 MeV) energies, large discrepancies between the different data sets are observed.

The calculation of the correlation matrix is in progress. It might give some information on the reason for these discrepancies.

In Fig. 3, the energy dependence of evaluated DN yield data for ^{237}Np from the ENDF/B-VII [6] and JEFF-3.2 [7] libraries are compared to experimental data. Obviously, the library data deviate from the experimental data of the present work. Those libraries seem to be based on Uranium data for which the DN energy dependence has a special trend. In Fig. 4, a plateau at low energy (<4 MeV) linked to another plateau at high energy (>6 MeV) (with lower DN values) with a linear slope is observed [5,6] for ^{238}U. A similar trend is seen for other isotopes of Uranium and Plutonium [6].

The difference between Uranium and Plutonium isotopes from one side and Neptunium from the other side could result from the even-odd effect. In fact, ^{237}Np has an odd number of protons ($Z = 93$). Therefore, the increase of the excitation energy (up to the opening of the channel for second chance fission) could lead to more excited fragments which finally produce less neutron-rich fission products. Hence, fewer DN precursors could be produced. For even Z fissioning nucleus, the increase of excitation energy could allow the breaking of some proton pairs, producing more odd Z fragments. Since delayed neutron precursors have mainly odd Z values, the number of precursors would not decrease for these even Z fissioning nuclei, on contrary to the Np case which has an odd Z value. These assumptions will be verified in future work by comparing experimental data to results of different modelling codes. Comparisons to FIFRELIN [8] and GEF [9] codes are in progress.

5. Conclusion

The absolute DN yields for ^{237}Np were measured for neutron energies from 1.5 MeV up to 16 MeV. The neutron detector was made up of 12 ^{3}He counters placed in a polyethylene cylinder. Neutron fields with special structures were used to maintain the equilibrium and obtain the required statistics.

In contrast to the U and Pu isotopes, the energy dependence of the present experimental DN yields does not show a step behaviour but a smooth decrease. This result is in rather good agreement with data from the literature, except for energies below 2 MeV, but very different from those of the ENDF/B-VII and JEFF-3.2 libraries.

The uncertainty bars for the DN yields have been obtained by propagating all the uncertainties. The calculation of the correlation matrix is in progress.

This work was supported by the EURATOM 7 Framework Programme ERINDA. We would also like to thank the staff of the PTB Ion Accelerator Facility for providing the beams and the support during the measurements.

DOI: 10.1051/epjconf/201714604029

References

[1] X. Ledoux et al., Annals of Nucl. Energy **76**, 514–520 (2015)
[2] R. Nolte et al., Radiat. Prot. Dosim **110**, 97–102 (2004)
[3] D.B. Pelowitz, MCNPX User's Manual Version 2.5.0 Los Alamos National Laboratory report LA-CP-05-0369 (April 2005)
[4] EXFOR, Experimental Nuclear Reaction Data, Nucl. Data Sheets **120**, 272 (2014)
[5] Delayed neutron data for the major actinides, NEA/WPEC-6, OECD 2002
[6] ENDF/B-VII, Evaluated Nuclear Data File, available on `http://www.nndc.bnl.gov`
[7] JEFF-3.2, Joint Evaluated Fission and Fusion File, OECD/NEA available on `https://www.oecd-nea.org/dbdata/`
[8] O. Litaize et al., EPJA **51**, 177 (2015)
[9] K.H. Schmidt et al., Nucl. Data Sheets **131**, 107 (2016)